In situ generation Ni/Fe hydroxide layers by anodic etching of Ni/Fe film for efficient oxygen evolution reaction

Ling Li[a], Jing Wu[a,b], Lieyuan Huang[a], Gaoli lan[a], Naxiang Wang[a], Hui Zhang[a], Xin Chen[a], Xingbo Ge[a,c]*

a *School of Chemistry and Chemical Engineering, Southwest Petroleum University, Chengdu, Sichuan 610500, P. R. China*

b *China Petroleum Pipeline Research Institute CO., LTD, Langfang, Hebei 065000, P. R. China*

c *Oil & Gas Field Applied Chemistry Key Laboratory of Sichuan Province, Southwest Petroleum University, Chengdu, Sichuan 610500, P. R. China*

*Corresponding author.

Email: xbge@swpu.edu.cn; Fax: 86-28-83037337; Tel: +86-28-83037337

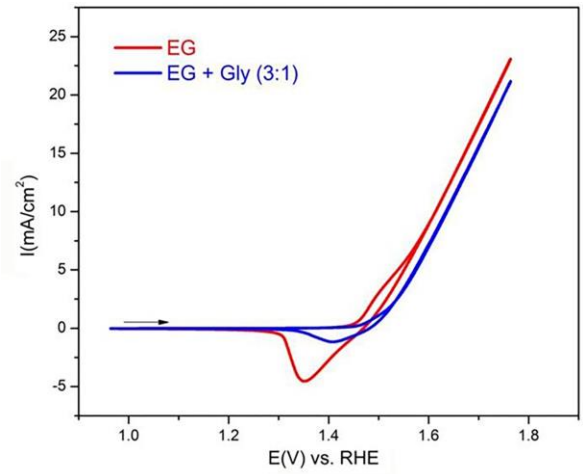

Figure S1. Effect of glycerol (Gly) in electrolyte studied by CV in 0.1 M KOH (scan rate of 20 mV s^{-1}).

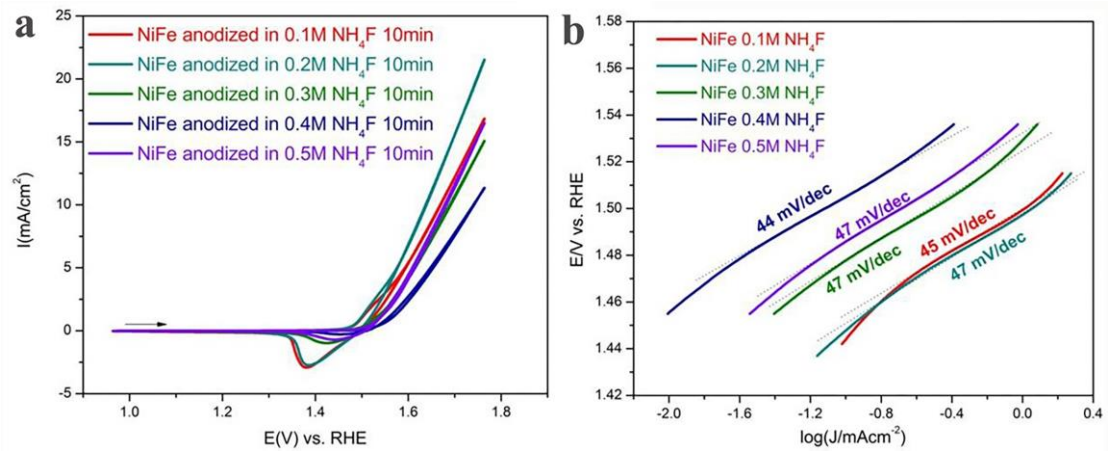

Figure S2. (a) CV curves and (b) Tafel plots of the different concentration of NH_4F in 0.1 M KOH (scan rate of 20 mV s^{-1}).

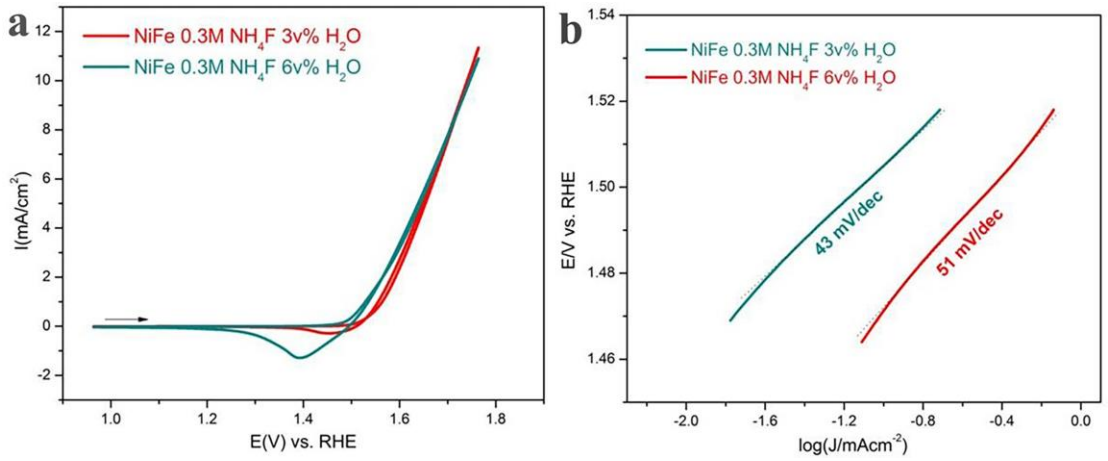

Figure S3. (a) CV curves and (b) Tafel plots of the different concentration of H_2O in 0.1 M KOH (scan rate of 20 mV s^{-1}).

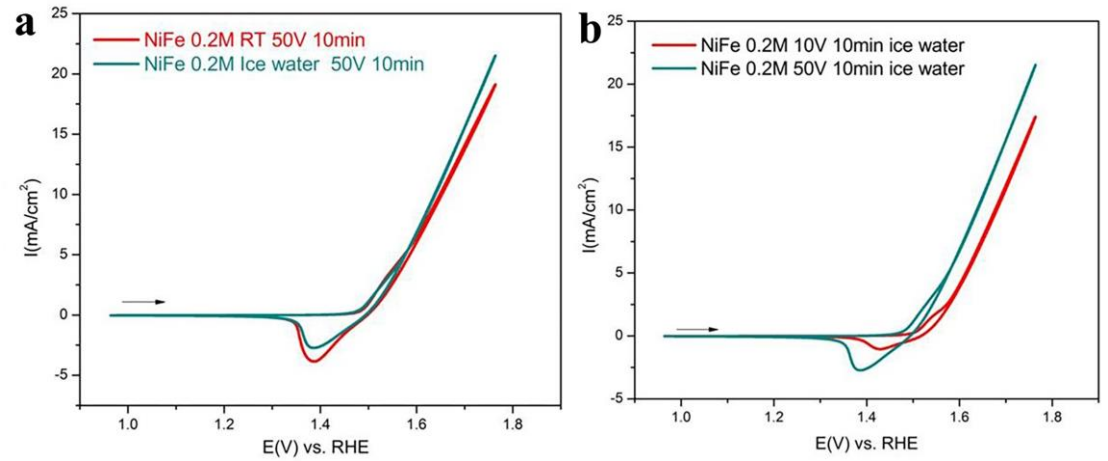

Figure S4. Effect of (a) temperature and (b) potential value during the anodization process studied by CV in 0.1 M KOH (scan rate of 20 mV s^{-1}).

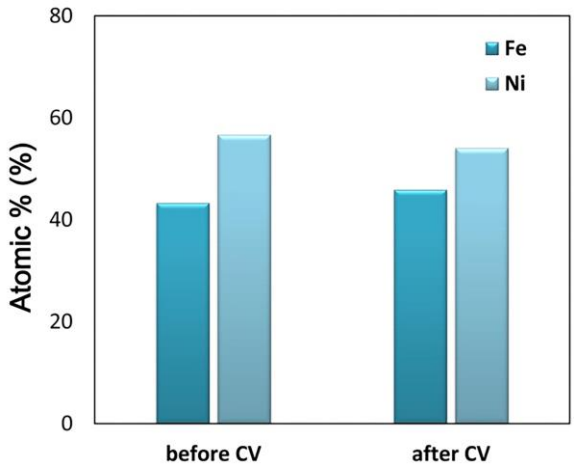

Figure S5. EDS results of fluorinated Ni/Fe (before CV treatment) and Ni/Fe hydroxide layers (after CV treatment).

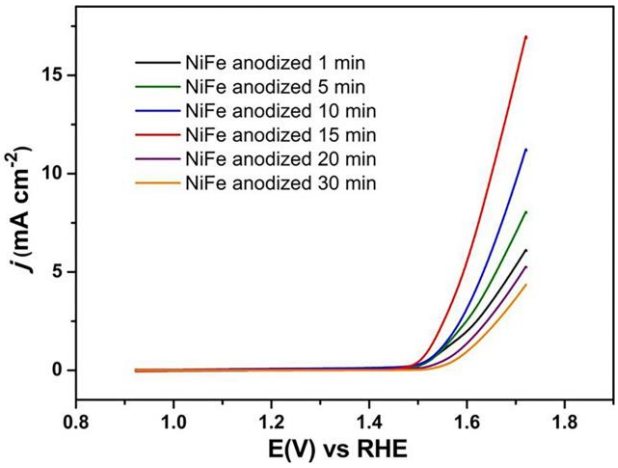

Figure S6. CV curves of the different anodizing time of NiFe alloy in 0.1 M KOH (scan rate of 20 mV s^{-1}).

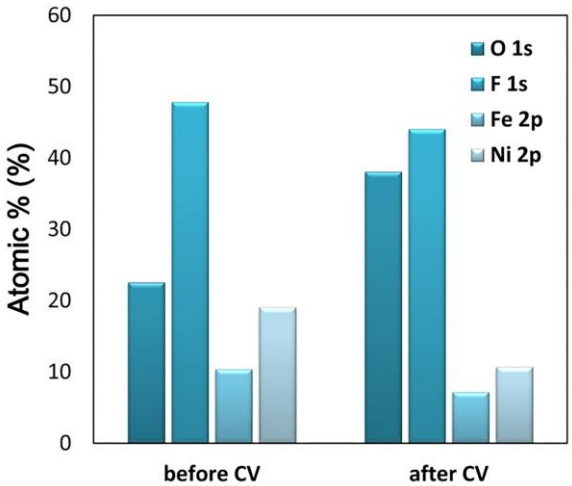

Figure S7. XPS results of surface atomic% of fluorinated Ni/Fe (before CV treatment) and Ni/Fe hydroxide layers (after CV treatment).

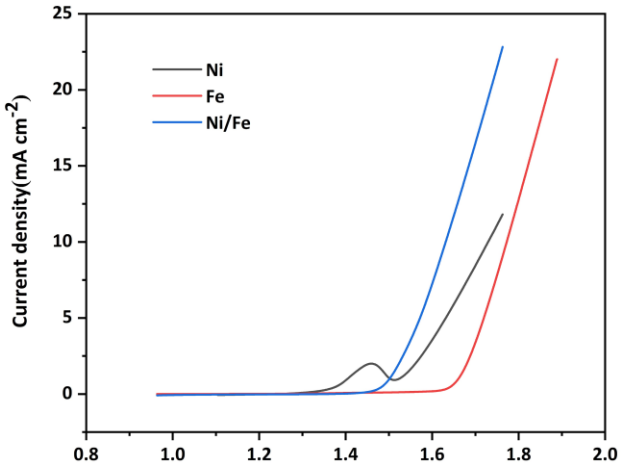

Figure S8. LSV polarization curves of Ni (the grey), Fe (the red) and Ni/Fe (the blue) under anodization and CV treatment for OER electrocatalytic activity in 0.1 M KOH.

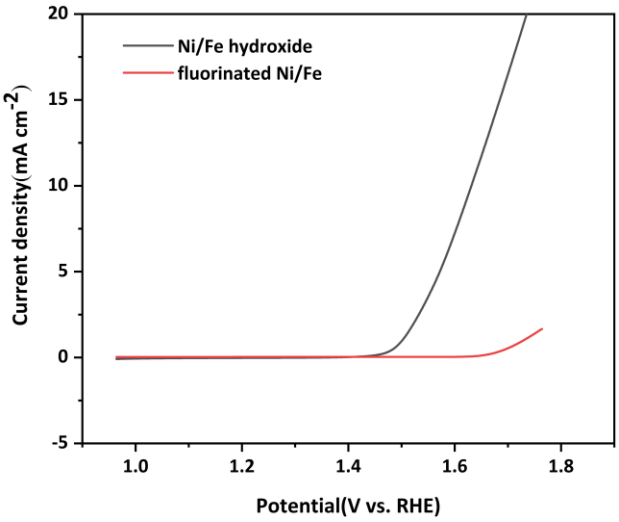

Figure S9. LSV polarization curves of Ni/Fe hydroxide and fluorinated Ni/Fe for OER electrocatalytic activity in 0.1 M KOH.

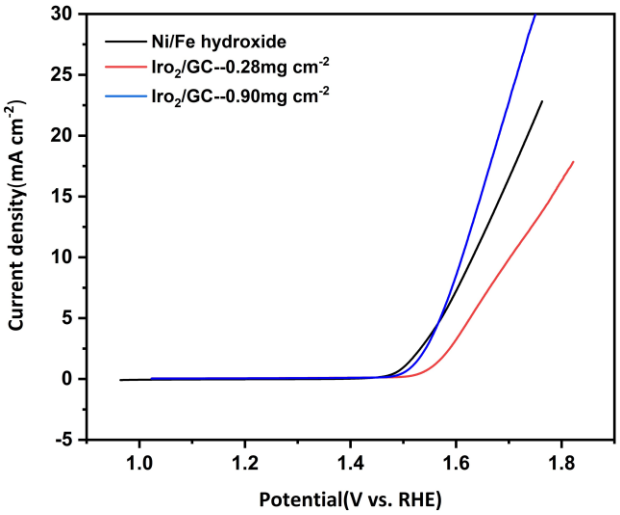

Figure S10. LSV polarization curves of Ni/Fe hydroxide (the black) and IrO_2 (loading mass: 0.90 mg cm^{-2} (the blue), 0.28 mg cm^{-2} (the red)) for OER electrocatalytic activity.

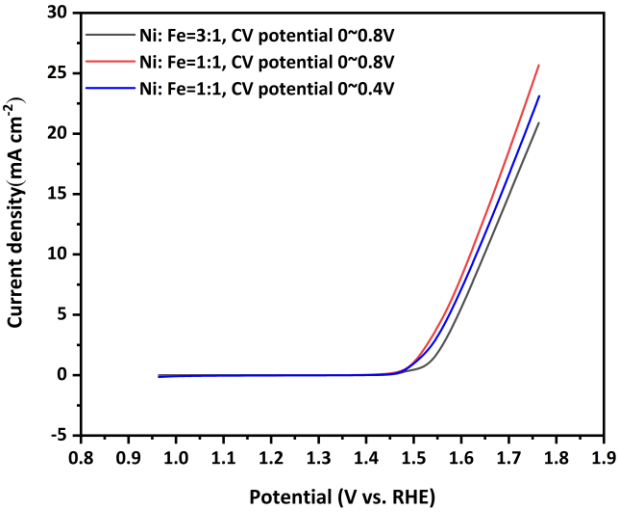

Figure S11. Effect of different Ni hydroxide/Fe hydroxide ratio for OER electrocatalytic activity studied by LSV in 0.1 M KOH.

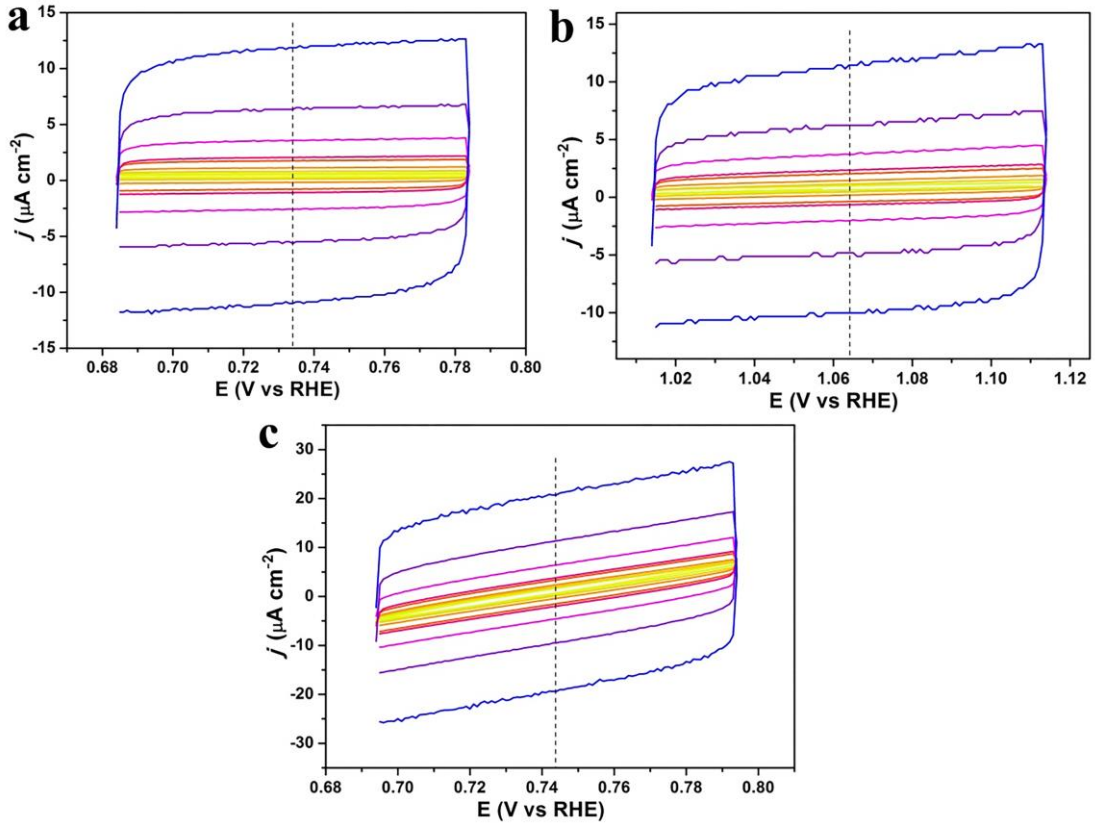

Figure S12. Capacitive CV of (a) NiFe alloy, (b) fluorinated Ni/Fe and (c) Ni/Fe hydroxide recorded at different scan rates, where no apparent faradaic process has taken place.

Table S1. Selected summary of NiFe-based OER catalyst.

Catalyst	Electrolyte	η (mV)	Tafel slop (mV dec^{-1})	Ref.
Ni/Fe hydroxide	0.1 M KOH	240	47	This work
NiHCF	0.1 M KOH	364	50	[1]
Ni/Fe-150	0.1 M KOH	341	68	[1]
Ni/Fe-300	0.1 M KOH	310	44	[1]
Ni/Fe-450	0.1 M KOH	342	57	[1]
Ni/Fe-600	0.1 M KOH	370	69	[1]
$Sr_2Fe_{1.3}Ni_{0.2}Mo_{0.5}O_{6-\delta}$	0.1 M KOH	360	59	[2]
NiFe-SW	1 M KOH	220	38.9	[3]
Ni–Fe LDH DSNCs	1 M KOH	272	71	[4]
$NiFeO_x(OH)_y$	1 M KOH	250	39	[5]
FeOOH/LDH	1 M KOH	174	46	[6]

Table S2. XPS results of the Ni/Fe ratio with different samples.

Samples	Atomic (%)	
	Ni	Fe
Ni: Fe=1:1, CV potential 0~0.8V	55.42	44.58
Ni: Fe=3:1, CV potential 0~0.8V	89.53	10.47
Ni: Fe=1:1, CV potential 0~0.4V	59.14	40.86

References

1. L. Y. Huang, X. B. Ge and S. Dong, *RSC Adv.*, 2017, 7, 32819-32825.
2. K. Zhu, T. Wu, M. Li, R. Lu, X. Zhu and W. Yang, *J. Mater. Chem. A.*, 2017, 5, 19836.
3. W. Zhang, Y. Z. Wu, J. Qi, M. X. Chen and R. Cao, *Adv. Energy Mater.*, 2017, 7, 1602547.
4. J. Zhang, L. Yu, Y. Chen, X. F. Lu, S. Gao and X. W. Lou, *Adv. Mater.* 2020, 32, 1906432.
5. H. Liao, P. Tan, R. Dong, M. Jiang, et al., *J. Colloid. Interf. Sci.*, 2021, 591, 307-313.
6. J. Chen, F. Zheng, S. J. Zhang, A. Fisher, et al., *ACS Catal.*, 2018, 8, 11342-11351.